Molecular Mechanism of Photosynthetic Oxygen Evolution: A Theoretical Approach

Davide M. Proserpio,[†] Roald Hoffmann,*[,†] and G. Charles Dismukes[‡]

Contribution from the Department of Chemistry and Materials Science Center, Cornell University, Ithaca, New York 14853-1301, and The Henry H. Hoyt Laboratory, Princeton University, Princeton, New Jersey 08544-1009. *Received August 19, 1991*

Abstract: Possible mechanisms for O_2 evolution in photosystem II (PSII) are studied with a semiempirical one-electron molecular orbital procedure, the extended Hückel method. The oxygen coupling is examined starting from some known inorganic complexes of manganese. Idealized geometries of four binuclear complexes (two di-μ-oxo, one tri-μ-oxo and one μ-carboxylato-di-μ-oxo) are distorted to transform into O_2-bound complexes. The computed Walsh diagrams are analyzed. For these structures the predicted oxidation to dioxygen is energetically unfavorable and would require two two-electron steps forming bound peroxide as an intermediate. An in-plane approach of two oxo ligands has a lower barrier for peroxide bond formation. Four tetranuclear Mn clusters are built combining binuclear complexes, a Mn_4O_4 cubane-like core, three $(Mn_2O_2)_2(\mu\text{-}O_2)$ "dimer of dimers" cores with $\mu_4,\eta^2\text{-}O_2$ bound either in or out of the Mn_4 plane formed by two parallel Mn_2O_2 units, and a "planar T" combination of two orthogonal Mn_2O_2 units with a Mn_3O_2 core and $\mu_3,\eta^2\text{-}O_2$ bound to three Mn atoms. The assumed pathway leading to peroxide bond formation in each of these is found to have appreciably lower energy for the $(Mn_2O_2)_2(\mu\text{-}O_2)$ and the "planar T" models with in-plane O–O approach. A slight energetic advantage is calculated in the peroxide to dioxygen step when the oxo ligands are coordinated to at least three Mn ions compared to coordination to only two Mn ions. Qualitative valence bond analysis indicates that release of symmetrically coordinated dioxygen, as in *cis*- and *trans*-μ-O_2, requires overcoming an ~1-eV electronic barrier for formation of ground-state O_2 (triplet). The tetranuclear models are introduced into speculative mechanisms and compared with current knowledge of the photosynthetic water oxidation reaction.

Introduction

The mechanism of O_2 evolution in photosystem II (PSII)[1] is typically discussed in terms of the so-called "S-states". The model is based on a measurement of O_2 release after a series of short flashes of light,[2] so that, in each reaction center, there is a single charge separation event taking place per flash. The yield of O_2 in response to short flashes of light shows a characteristic oscillation pattern with a periodicity of four flashes. To account for this result, it was proposed[2b] that PSII cycles through five states (S_0–[S_4]), I.

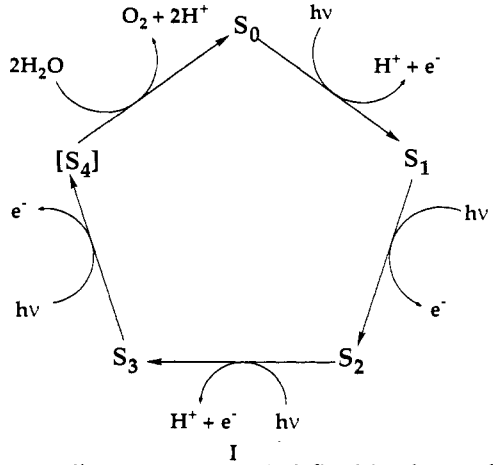

I

The intermediate states are each defined by the number of electrons extracted from the water-oxidizing complex of PSII.

The species which is oxidized in each of the S transitions appears to be a tetramanganese cluster, except possibly for the $S_2 \rightarrow S_3$ transition, where something other than manganese may be oxidized. The identity of this other species is unknown, although electron paramagnetic resonance (EPR) evidence has implicated a protein residue close to the Mn cluster,[3a-d] possibly a histidine residue.[3e]

The S_0 and S_1 states are stable essentially indefinitely, depending on the pH, while S_2 and S_3 are unstable and decay be reduction to S_1 on the time scale of several seconds to minutes. After four electrons are extracted, the unstable [S_4] state is created and reverts to S_0 within 1 ms with simultaneous release of a molecule of O_2. After a period of dark adaptation, the S states reach a steady-state distribution of 75% S_1 and 25% S_0, which quantitatively accounts for the flash yield of O_2. The measured yield of proton release[4] is known to be modulated in a pattern of 1, 0, 1, 2 as the cycle progresses from S_0 back to S_0, considering $S_3 \rightarrow [S_4] \rightarrow S_0$ as one step.

One essential feature of scheme I is that, during the $S_0 \rightarrow S_3$ transitions, water is not oxidized. Water oxidation apparently takes places only after the third step, in one concerted four-electron reaction or two two-electron reactions.[5] That water is oxidized only in [S_4] is suggested also by the fact that $H_2{}^{18}O$ can still be exchanged with $H_2{}^{16}O$ in the S_3 state.[6] This result, based on mass-spectrometric analysis of O_2 gas, has been challenged on the basis that the method used was not rapid enough to permit

[†] Cornell University.
[‡] Princeton University.

(1) For recent reviews, see: (a) Hansson, O.; Wydrzynski, T. *Photosynth. Res.* **1990**, *23*, 131-162. (b) Ghanotakis, D. F.; Yocum, C. F. *Annu. Rev. Plant Physiol. Plant Mol. Biol.* **1990**, *41*, 255-276. (c) Vincent, J. B.; Christou, G. *Adv. Inorg. Chem.* **1989**, *33*, 197-257. (d) Brudvig, G. W.; Crabtree, R. H. *Prog. Inorg. Chem.* **1989**, *37*, 99-142. (e) Brudvig, G. W.; Beck, W. F. *Annu. Rev. Biophys. Biophys. Chem.* **1989**, *18*, 25-46. (f) Volkov, A. G. *Bioelectrochem. Bioenerg.* **1989**, *21*, 3-24. (g) Rutherford, A. W. *Trends Biochem. Sci.* **1989**, *14*, 227-232. (h) Renger, G. *Angew. Chem., Int. Ed. Engl.* **1987**, *26*, 643-660. (i) Renger, G. *Photosynthetica* **1987**, *21*, 203-224. (j) Babcock, G. T. In *New comprehensive Biochemistry: Photosynthesis*; Amesz, J., Ed.; Elsevier: New York, 1987; pp 125-158. (k) Dismukes, G. C. *Photochem. Photobiol.* **1986**, *43*, 99-115. (l) Govindjee. *Mendeleev Chem. J. (Engl. Transl.)* **1986**, *31*, 52-73. (m) Renger, G.; Wydrzynski, T. *Biol. Met.* **1991**, *4*, 73-80. (n) Govindjee; Coleman, W. J. *Sci. Am.* **1990**, 50-58. (o) Thorp, H. H.; Brudvig, G. W. *New J. Chem.* **1991**, *15*, 479-490.

(2) (a) Joliot, P.; Barbieri, G.; Chabaud, R. *Photochem. Photobiol.* **1969**, *10*, 309-329. (b) Kok, B.; Forbush, B.; McGloin, M. *Photochem. Photobiol.* **1970**, *11*, 457-475.

(3) (a) Boussac, A.; Zimmermann, J.-L.; Rutherford, A. W. *Biochemistry* **1989**, *28*, 8984-8959; *FEBS Lett.* **1990**, *227*, 69-74. (b) Sivaraja, M.; Tso, J.; Dismukes, G. C. *Biochemistry* **1989**, *28*, 9459-9464. (c) Tso, J.; Sivaraja, M.; Dismukes, G. C. *Biochemistry* **1991**, *30*, 4734-4739. (d) Tso, J.; Sivaraja, M.; Philo, J. S.; Dismukes, G. C. *Biochemistry* **1991**, *30*, 4740-4747. (e) Boussac, A.; Zimmermann, J.-L.; Rutherford, A. W.; Lavogne, J. *Nature* **1990**, *397*, 303-306.

(4) (a) Förster, V.; Junge, W. *Photochem. Photobiol.* **1985**, *41*, 183-190. (b) Saygin, Ö; Witt, H. T. *Photobiochem. Photobiophys.* **1985**, *10*, 71-81.

(5) (a) Krishtalik, L. I. *Biochim. Biophys. Acta* **1986**, *849*, 162-171. (b) Brudvig, G. W.; dePaula, J. C. In *Progress in Photosynthesis Research*; Biggins, J., Ed.; M. Nijhoff: Boston, 1987; Vol. 1, pp 491-498. (c) Krishtalik, L. I. *Bioelectrochem. Bioenerg.* **1990**, *23*, 249-263.

(6) (a) Radmer, R.; Ollinger, O. *FEBS Lett.* **1986**, *195*, 285-289. (b) Bader, K. P.; Thibault, P.; Schmid, G. H. *Biochim. Biophys. Acta* **1987**, *893*, 564-571.

0002-7863/92/1514-4374$03.00/0

examination of the unstable S_2 and S_3 states.[1i]

It is generally agreed that, stoichiometrically, four manganese ions are associated as an indispensable cofactor with each PSII unit, but the question of how the metal ions organize within the protein is still the subject of considerable debate.

Recently X-ray absorption spectroscopy (XAS) has provided further information about the structural arrangement of the Mn ions.[7] Data have been obtained for the S_1, S_2, and S_3 states. Indirect information on the S_0 state is extracted from study of the S_0* state induced by hydroxylamine. Analysis of these data indicates that each Mn possesses 4–6 N or O atoms between 1.8 and 2.2 Å, 1–1.5 (1.3–2.9, ref 7a) Mn atoms at 2.7 Å,[7d,g] and 0.5 (0.5–1.1, ref 7a; 0.5–1, ref 7d) Mn or Ca atoms at 3.3 Å.[7g] Another scattering shell may be present from a heavy atom at >4.2 Å, hypothesized to be due to Ca.[7d] The first shell of light atom scatterers possibly may be resolved into 2 O/N at 1.8 Å and 2–4 O/N at 1.9–2.1 Å.[7b,c] EPR and ESEEM (electron spin echo envelope modulation) studies support the predominance of oxygen as a ligand.[8] The latter technique has implicated one or more nitrogen atoms to be in hydrogen-bonding contact with the Mn cluster or possibly directly coordinated.[9] Chemical modification of amino acid residues in PSII has pointed to histidine and carboxylate residues as interacting with the Mn cluster, possibly as Mn ligands.[10] Also, site-directed mutagenesis has implicated glutamic and aspartate residues as being essential for stable water oxidation, although their roles are unclear.[11]

Assuming that the Mn coordination number is similar to that of mononuclear complexes, a total of 24 ligand atoms in the cluster would be expected. This number should be reduced by one for each μ-oxo and by two for each μ_3-oxo bridge.

The short Mn–Mn distance of 2.7 Å exists in all the known di-μ-oxo and di-μ-oxo-mono-μ-carboxylato structures of binuclear complexes of manganese,[12] which also exhibit a short 1.8–1.9-Å Mn–O distance. In Mn clusters the 3.1–3.3-Å separation is exemplified by a wider range of possible ligand types. Particularly relevant are the dinuclear mono-μ-oxo and the trinuclar tri-μ-oxo manganese complexes, both of which possess a single oxo atom bridge and a pair of bidentate μ-carboxylato bridges.[12] These compounds are stable in aqueous acidic solutions.

Only subtle changes in the EXAFS (X-ray absorption fine structure) spectrum are found to accompany the $S_1 \rightarrow S_2 \rightarrow S_3$ transitions, indicating that no significant rearrangement of ligands occurs in these steps.[7b] However, structural changes are found for the S_0* state induced by hydroxylamine, suggesting that the same would be true for the S_0.[7c] The EPR and XAS studies[7] also propose an average oxidation state of +3 for manganese in the S_1 state.

EXAFS dichroism data on an oriented PSII membrane has revealed a high degree of order for the 3.3-Å Mn–Mn vector which is located parallel to the normal of the photosynthetic membrane. The 2.7-Å Mn–Mn vector which is oriented orthogonally to the 3.3-Å vector exhibits considerably less dichroism.[7a,g] Taken together this suggests a minimal model in which two short (2.7 Å) di-μ-oxo binuclear Mn pairs are linked by a longer mono-μ-oxo bridge (3.3 Å) to form a tetranuclear cluster, as indicated in II. Of the two possible geometries noted in II, the more symmetrical geometry on the left would agree with the linear dichroism results for the Mn EXAFS.[7a,g] It is important to note, however, that it is not possible to eliminate distorted cubane-like, bent linear, or trinuclear models on the basis of the XAS data alone. Recent EPR[13] and magnetic susceptibility[14] results for the S_2 state have eliminated the model in which a mononuclear manganese center is involved in redox reactions.

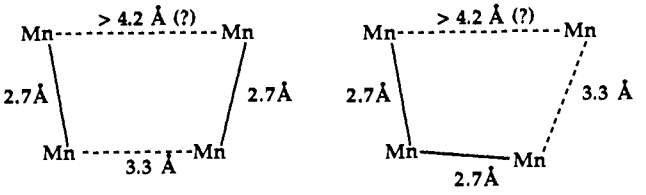

II

No structural information is available for the unstable [S_4] state, which is responsible for the release of oxygen.

As far as we know, under homogeneous conditions, none of the synthetic binuclear nor tetranuclear clusters made to date has been found capable of oxidizing water and evolving O_2. On the other hand, in heterogeneous suspensions of the di-μ-oxo dimer $(bpy)_2Mn(O)_2(bpy)_2$, composed of a saturated aqueous solution in contact with the solid, it has been reported that illumination does produce some O_2, albeit inefficiently.[15a] The active species is unknown but almost certainly is not an isolated dimer. This is also true for the chemical and photolytic oxidation of water by heterogeneous suspensions of "activated" MnO_2.[15b] "Activation" of the unreactive rutile form of MnO_2 occurs by sonication or dispersion within micelles, presumably reflecting formation of new centers which are stronger oxidants or better suited to O–O bond formation.

The Models. Let's first examine the basic electronic difficulties in O–O coupling by considering two O^{2-} ions. As they approach each other, their levels will combine in a characteristic pattern with all the antibonding combinations filled (see III). In order to switch on any bonding interaction, we must remove some electrons from the higher $2\sigma_u$* and π_g* levels, i.e., oxidize the system.

A simplistic approach to the problem might begin by neglecting the two long Mn···Mn contacts in II, and considering the possibility of O–O bond formation in a di-μ-oxo binuclear complex. We probe this possibility by a semiempirical one-electron molecular orbital procedure, the extended Hückel method. Levels are calculated and then filled with electrons. The method is not good at calculating absolute energy differences between states, but models general orbital energy trends and major charge shifts well. In the case at hand, where predicting differences between Mn oxidation states such as Mn(III) and Mn(IV) is the goal, the method is particularly vulnerable. It is within the spirit of the method to assume the same parameters for all oxidation states

(7) (a) George, G. N.; Prince, R. C.; Cramer, S. P. *Science* **1989**, *243*, 789–791. (b) Guiles, R. D.; Zimmermann, J.-L.; McDermott, A. E.; Yachandra, V. K.; Cole, J. L.; Dexheimer, S. L.; Britt, R. D.; Wieghardt, K.; Bossek, U.; Sauer, K.; Klein, M. P. *Biochemistry* **1990**, *29*, 471–485. (c) Guiles, R. D.; Yachandra, V. K.; McDermott, A. E.; Cole, J. L.; Dexheimer, S. L.; Britt, R. D.; Bossek, U.; Sauer, K.; Klein, M. P. *Biochemistry* **1990**, *29*, 486–496. (d) Penner-Hahn, J. E.; Fronko, R. M.; Percoraro, V. L.; Yocum, C. F.; Betts, S. D.; Bowlby, N. R. *J. Am. Chem. Soc.* **1990**, *112*, 2549–2557. (e) Kusunoki, M.; Ono, T.; Matsushita, T.; Oyanagi, H.; Inoue, Y. *J. Biochem.* **1990**, *108*, 560–567. (f) Yachandra, V. K.; DeRose, V. J.; Latimer, M. J.; Mukerji, I.; Sauer, K.; Klein, M. P. *Photochem. Photobiol.* **1991**, *53S*, 98S. (g) Sauer, K.; Yachandra, V. K.; Britt, R. D.; Klein, M. P. In *Manganese Redox Enzymes*; Pecoraro, V. L., Ed.; VCH Publishers: New York, in press.

(8) (a) Hansson, O.; Andréasson, L.-E.; Vanngard, T. *FEBS Lett.* **1986**, *195*, 151–154. (b) Britt, R. D.; DeRose, V. J.; Yachandra, V. K.; Kim, D.; Sauer, K.; Klein, M. P. In *Current Research in Photosynthesis*; Baltscheffsky, M., Ed.; Kluwer Academic Press: Dordrecht, 1990; Vol. I, pp 769–772.

(9) DeRose, V. J.; Yachandra, V. K.; McDermott, A. E.; Britt, R. D.; Sauer, K.; Klein, M. P. *Biochemistry* **1991**, *30*, 1335–1341.

(10) (a) Tamura, N.; Ikeuchi, M.; Inoue, Y. *Biochim. Biophys. Acta* **1989**, *973*, 281. (b) Seibert, M.; Tamura, N.; Inoue, Y. *Biochim. Biophys. Acta* **1989**, *974*, 185–191. (c) Ono, T.-A.; Inoue, Y. *FEBS Lett.* **1991**, *278*, 183–186.

(11) (a) Vermaas, W.; Charité, J.; Shen, G. *Biochemistry* **1990**, *29*, 5325–5332. (b) Nixon, P. J.; Diner, B. A. In *Proc. 17th IEEE: Engineering in Medicine and Biology Society*; Pedersen, P. C., Onaral, B., Eds.; IEEE: New York, 1990; pp 1732–1734. (c) Preston, C.; Seibert, M. In *Current Research in Photosynthesis*; Baltscheffsky, M., Ed.; Kluwer Academic Press: Dordrecht, 1990; Vol. I, pp 925–928.

(12) For recent reviews on the inorganic models, see: (a) Que, L., Jr.; True, A. E. *Prog. Inorg. Chem.* **1990**, *38*, 98–200. (b) Wieghardt, K. *Angew. Chem., Int. Ed. Engl.* **1989**, *28*, 1153–1172. (c) Christou, G. *Acc. Chem. Res.* **1989**, *22*, 328–335. (d) Pecoraro, V. *Photochem. Photobiol.* **1988**, *48*, 249–264.

(13) Kim, D. H.; Britt, R. D.; Klein, M. P.; Sauer, K. *J. Am. Chem. Soc.* **1990**, *112*, 9389–9390.

(14) Sivaraja, M.; Philo, J. S.; Lary, J.; Dismukes, G. C. *J. Am. Chem. Soc.* **1989**, *111*, 3221–3225.

(15) (a) Ramaraji, R.; Kira, A.; Kaneko, M. *Angew. Chem., Int. Ed. Engl.* **1986**, *25*, 825–827. (b) Luneva, N. P.; Shafirovich, V. Ya.; Shilov, A. E. *J. Mol. Catal.* **1989**, *52*, 49–62.

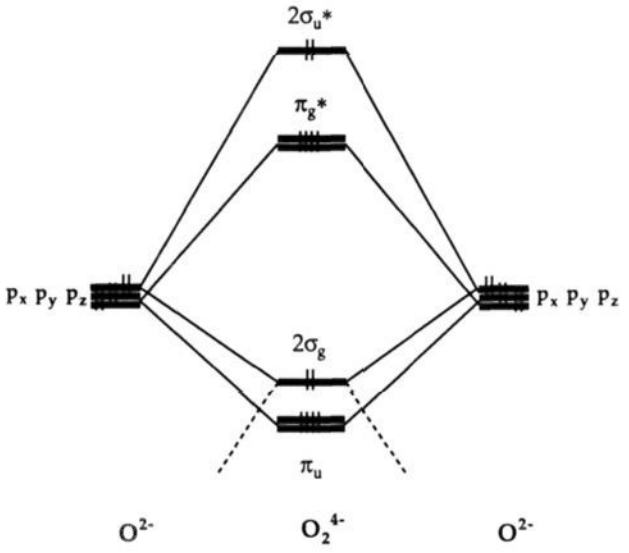

III

of a transition metal and look for differences only due to electron occupation (vide infra). Computational details are given in the Appendix.

To mimic the S_3 and $[S_4]$ states we focus our attention on the structural constraints that favor the oxygen coupling. We model a simplified tetramanganese complex with idealized geometry, and then we compute a possible distortion that transforms the original structure into an O_2-bound complex. Two limiting structures are considered, one of which is modeled on known inorganic complexes. The oxidation state of Mn is assumed to be formally four, and the O–O separation for the final compound is set to 1.3 Å, intermediate between those of O_2 and O_2^{2-}. We adopt the hypothesis that the initial dioxo species forms in the $[S_4]$ state.

We first build a binuclear model with two manganese atoms separated by 2.7 Å. This short distance can be supported by two *oxo bridges with Mn–O 1.8 Å, found in inorganic complexes* possessing the di-μ-oxo or di-μ-oxo-mono-μ-carboxylato ligands (see ref 12). For terminal ligands, we choose H_2O, Mn–O 2.1 Å. Our first model, $[Mn^{IV}_2(\mu\text{-}O)_2(H_2O)_8]^{4+}$ (**1a**) with D_{2h} symmetry, is shown in Figure 1. The easiest way to bring the two oxygens close to each other is to increase the length between the two Mn ions, keeping the four Mn–O bridging distances constant, until we reach the O–O distance of 1.3 Å (see Figure 1). The final product is $[Mn^{III}_2(\mu,\eta^2\text{-}O_2)(H_2O)_8]^{4+}$ (**1b**).

In Figure 2 we show the computed Walsh diagram along this distortion. We distinguish four regions. Starting from the top, between −7.8 and −9.6 eV, there are four unoccupied levels. Considering our model as derived from two octahedra sharing one edge, these high levels are descending from the "e_g" sets (d_{z^2}, $d_{x^2-y^2}$). The region between −11.5 and −12.3 eV (d-block) is characterized by six levels deriving from the two "t_{2g}" sets (d_{xy}, d_{xz}, and d_{yz}) of the edge-sharing octahedra. These half-filled levels are slightly pushed up by the ligands relative to the 5d orbitals in the free Mn(IV). The d-block remains almost unaffected along the distortion. Around the energy of the 2p orbitals of oxygen (−14.8 eV) are the oxygen lone pairs. Below −15.5 eV there are metal–ligand bonding molecular orbitals (MOs).

What are the relative energies of the $2\sigma_u^*$ and π_g^* levels, and does the proposed distortion lead to O–O bond formation? With the aid of a fragment molecular orbital analysis we project the contribution of these diatomic levels to the MOs of the whole molecule. In the geometry of **1a** in Figure 1 the $2\sigma_u^*$ and $\pi_g^*(z)$ orbitals start out unaffected as lone pairs on the oxo bridges. The long O···O distance of 2.4 Å does not yet induce significant antibonding repulsion. The x component of the π_g^* is distributed among three MOs: 67% in a MO mainly centered on the bridges (see Figure 2, left, and Figure 3, bottom left), 17% in a lower

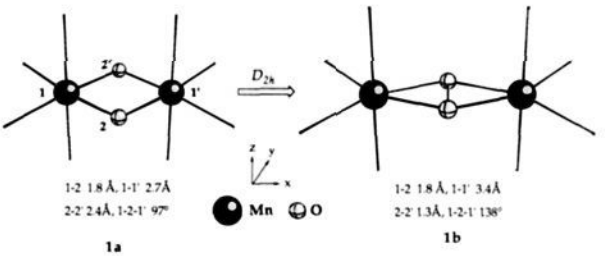

Figure 1. Model for the oxygen coupling in a binuclear Mn complex (**1**) with selected bond distances and angles.

Mn–O bonding MO, and 16% in the "e_g" set mainly centered on the Mn. The three MOs with major contributions of the parent $2\sigma_u^*$ and π_g^* are shown in Figure 3, where for clarity we omit the ligands above and below the plane and the hydrogens that do not contribute to the MOs.

As the oxygens move toward each other, at least one level has to go up and cross the metal d-block. The antibonding interaction between the approaching bridge atoms produces a rapid increase in energy of the $2\sigma_u^*$ level. The level crosses the d-block and mixes with the antisymmetric combination of the $d_{x^2-y^2}$ pair in the "e_g" set. Symmetry-avoided crossing (the dashed lines in Figure 2) yields a redistribution of the $2\sigma_u^*$ over three empty MOs. That there is an empty O–O antibonding orbital implies that a corresponding filled O–O bonding orbital is present, i.e., an O–O bond. In Figure 3 (upper right) we show only the antibonding MO with the largest oxygen contribution.

The π_g^* set is not so dramatically affected by the distortion. The z component contributes 77% to the level between the d-block and the O lone pair (see Figure 3, center right), and the remaining 23% mixes into the d-block. The x component redistributes over three MOs: 41% in a slightly Mn–O bonding MO (see Figure 3, bottom right), 22% in a Mn–O bonding orbital, and 29% in one of the MOs of the "e_g" set.

To compute the total energy along the distortion we have to consider how the electrons redistribute between the O^{2-} and Mn orbitals, thereby changing the spin multiplicity of two Mn(IV) d^3 high-spin ions. We start populating the six levels from the "t_{2g}" sets with six unpaired electrons (see IV, left), modeling Mn^{IV}_2 high spin ($S = 3$). The left-hand side of this figure corresponds to a hypothetical state, the so-called "nascent" $[S_4]$ state, having the same number of electrons as the $[S_4]$ state, yet possessing the assumed structure of the S_3 state. As we move along the distortion we keep the highest multiplicity possible without occupying the antibonding Mn–O "e_g" set. This results in electronic redistribution from O^{2-} to Mn(IV) yielding 2Mn(III) with intermediate spin state $S = 2$ and a peroxo bridge. The resulting $[S_4]$ oxidation state is a precursor to the release of oxygen. This illustrates one of the electronic features presumed to be important for catalysis: the availability of nonbonding manganese orbitals of appropriate energy to accept electrons from the O^{2-} orbitals.

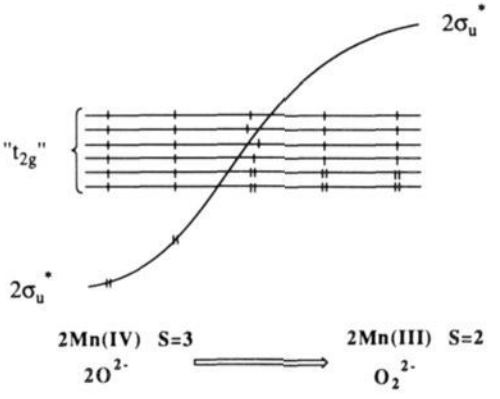

IV

The variation of the total energy, calculated for the occupations given in IV, is shown by a dashed line in the Walsh diagram of

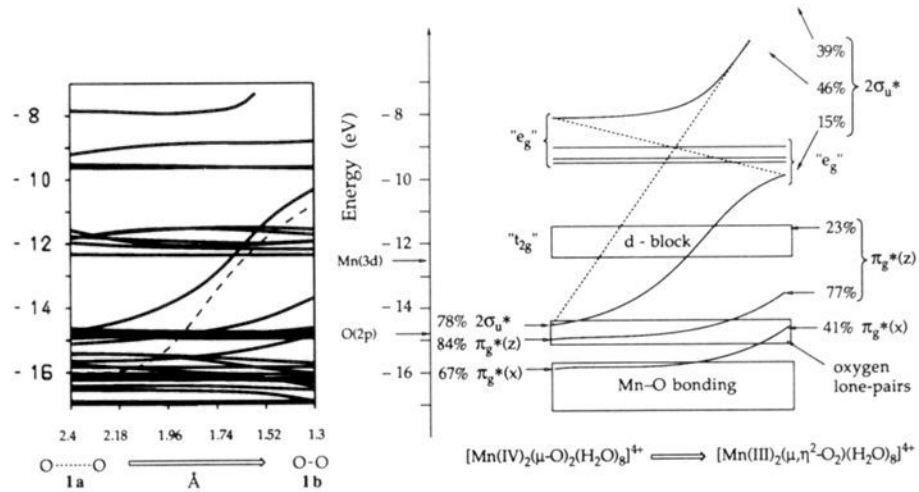

Figure 2. Walsh diagram for model **1**. See text.

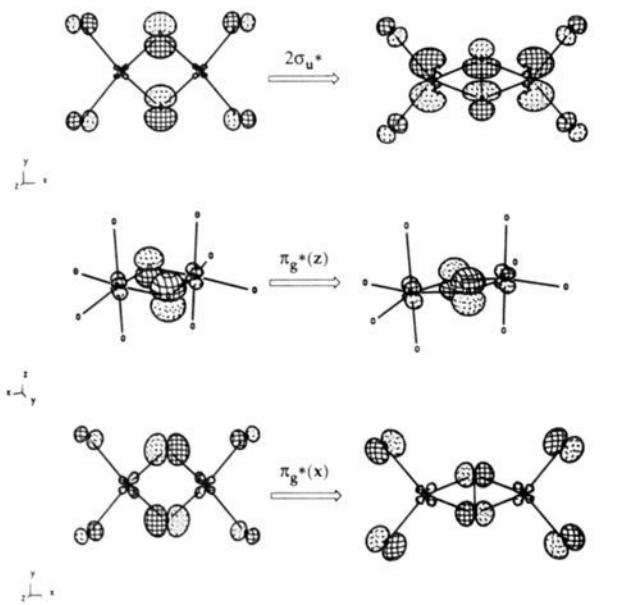

Figure 3. Selected MOs for distortion **1a–1b**. See text.

Figure 2 (the energy scale is the same as the levels). Note the high activation energy (5 eV); even given the quantitative unreliability of the extended Hückel theory, we think this model is an unrealistic one. The product is a symmetrically bridged peroxo complex (μ,η^2) of D_{2h} site symmetry, with a single O–O bond. To form a full O=O double bond, we have to remove two other electrons from the π_g^*. This is the inner $\pi_g^*(z)$ level, ~1.8 eV below the d-block in the last step, which carries the "holes" for the remaining two-electron oxidation. No wonder the total barrier is larger then 5 eV! This may be compared to the experimentally determined activation energy for the reaction $S_3 \rightarrow S_0 + O_2$ of 0.16 eV.[16]

Is it possible to lower this barrier within the binuclear model by inclusion of different ligands? We have done many calculations, with quite different types (H_2O, OH^-, and H^-) and arrangements of the ligands, trying to avoid eventual ligand–ligand repulsions. In no case were we able to reduce the barrier from its high value. Since we have shown in the Walsh diagram that the metal–terminal ligand interactions are not affected by the distortion (see Figures 1 and 2), in this case the substitution of H_2O or OH^- with the simpler H^- ligand (at 1.8 Å) is reasonable. This makes the comparison of different computed quantities (such as total energy, overlap population, and net charge) possible among different models, although the absolute values may not be reliable. One conclusion reached from this analysis is the high energetic stability of the planar Mn_2O_2 core. This may explain the strong preference for a planar Mn_2O_2 coordination in all the known di-μ-oxo-bridged complexes.[12]

To explore other possible elementary pathways for O–O bond formation we examine three different structures modeled by inorganic analogues, shown in Figure 4. $[Mn^{IV}_2(\mu\text{-}O)_3(H_2O)_6]^{2+}$ (**2a**, **2b**) mimics the tri-μ-oxo structure synthesized by Wieghardt et al.[17] This C_{3v} symmetry model (**2a**) presents three oxo bridges with Mn–O 1.8 Å and a short Mn–Mn distance of 2.3 Å. A C_{2v}

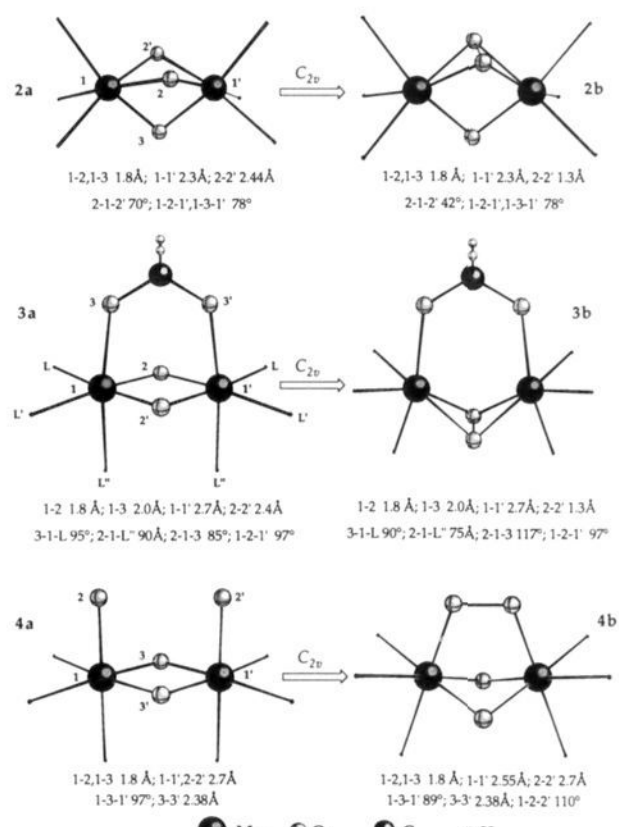

Figure 4. Models **2**, **3**, and **4** for the oxygen coupling in binuclear Mn complexes.

(16) Koike, H.; Hanssum, B.; Inoue, Y.; Renger, G. *Biochim. Biophys. Acta* **1987**, *893*, 524–533.

(17) Wieghardt, K.; Bossek, U.; Nuber, B.; Weiss, J.; Bonvoisin, J.; Corbella, M.; Vitols, S. E.; Girerd, J. J. *J. Am. Chem. Soc.* **1988**, *110*, 7389–7411.

Table I. Selected Overlap Populations (op) and Net Charges (nc) for the Structures Reported in Figures 1 and 4

model		op Mn–O[a]	op O–O[b]	nc Mn	nc O	ΔE (eV)
1a–1b	$[Mn_2(\mu\text{-}O)_2H_8]^{4-}$	0.41/0.31	0.00/0.54	+0.76/−0.20	−1.05/−0.13	4.50
2a–2b	$[Mn_2(\mu\text{-}O)_3H_6]^{4-}$	0.36/0.22	0.00/0.56	+1.03/+0.11	−1.16/−0.28	5.47
3a–3b	$[Mn_2(\mu\text{-}O)_2(\mu\text{-}H_2COO)H_6]^{3-}$	0.43/0.26	0.00/0.56	+1.35/+0.52	−1.01/−0.24	6.80
4a–4b	$[Mn_2(\mu\text{-}O)_2O_2H_6]^{6-}$	0.44/0.47	0.00/0.50	+0.91/−0.04	−1.52/−0.82	4.40

[a] For atoms 1–2 and 1′–2′ (see Figures 1 and 4). [b] Atoms 2–2′. Compare with op calculated at O–O 1.3 Å for O_2 (0.69) and O_2^{2-} (0.43).

distortion (**2b**) reduces the angle 2–1–2′ from 70° to 42° while keeping all the other distances constant. In **3a** and **3b** a new approach is tried, starting from a dimer $Mn^{IV}_2(\mu\text{-}O)_2(\mu\text{-}CH_2O_2)(H_2O)_6^{3+}$ with one μ-formate-κO:κO′ and two μ-oxo bridges (see ref 12). Here, the constraint of the μ-carboxylato does not allow the in-plane approach of the bridging oxo atoms. The out-of-plane approach changes the dihedral angle 1–2–2′–1′ from 180° to 107°, keeping Mn–O fixed at 1.8 Å. This distortion has been proposed as a possible step in the formation of O_2-bound species in PSII.[18]

The synthesis of the first binuclear $(\mu,\eta^2$-peroxo)dimanganese[19] suggests a different model for the oxygen coupling. A dimer, $Mn^{IV}_2(\mu\text{-}O)_2O_2(H_2O)_6$ with planar Mn_2O_2 core and *cis*-oxo ligands, is shown in **4a**. Bending the two fragments toward each other produces the μ,η^2-peroxo species **4b** (the dihedral angle 1–3–3′–1′ changes from 180° to 137°), which mimics the synthetic compound but with O–O 1.3 Å.

Table I reports the results of the different models **1–4**: the total energy variation (ΔE) between the two geometries with H^- terminal ligands; the Mn–O and O–O overlap populations (op); and the net charges (nc) on Mn and O. The op scale as bond orders: they are not 0, 1, and 2 as a chemist might like them, but they increase with increasing bond strength. Some typical values for O_2^- and O_2^{2-} are given for calibration. The Walsh diagrams (not reported here) for these complexes do not present new features compared to the one reported in Figure 2; the differences in total energy (ΔE) result principally from changes in the energy of the MOs involved in the oxygen bond.

It is difficult to choose the best model for oxygen coupling in a manganese dimer. Judging by the energy barrier, models **2a,b** and **3a,b** are disfavored. The formation of the O–O bond is less disfavored when the oxygens lie in the same plane as the metals. All the dimer models are unable to promote internal electron redistribution from the nascent $[S_4]$ state to $S_0 + O_2$, as judged by the energies of the π_g^* and Mn "t_{2g}" orbitals. This suggests that one of the possible functions of a tetrameric Mn site for water oxidation could be to lower the activation barrier for the formation of dioxygen. This will be explored later.

To complete our analysis of the possible geometries for dimers, we computed the energy barrier for the approach of two hexacoordinated Mn ions. This simple approach gives two structures not yet isolated. The first of these, as shown in the upper panel of Figure 5, brings two $MnOL_5$ units together such that coordinated oxo atoms can interact. The Mn ions are bound trans to the oxygens in a planar Mn_2O_2 core with C_{2h} symmetry. The oxygen bond coupling step involves translation of the two MnO centers along the O–O coordinate beginning at 2.7-Å and ending at 1.3-Å O–O separation. This gives an energy barrier of 6.5 eV. In the lower panel of Figure 5 the same complexes also approach along the O–O coordinate, but with a dihedral Mn–O–O–Mn angle of 90° and overall C_2 symmetry. The barrier is now 7.0 eV. These barriers are so high that significant translation of each $MnOL_5$ unit would be highly improbable. It suggests that the

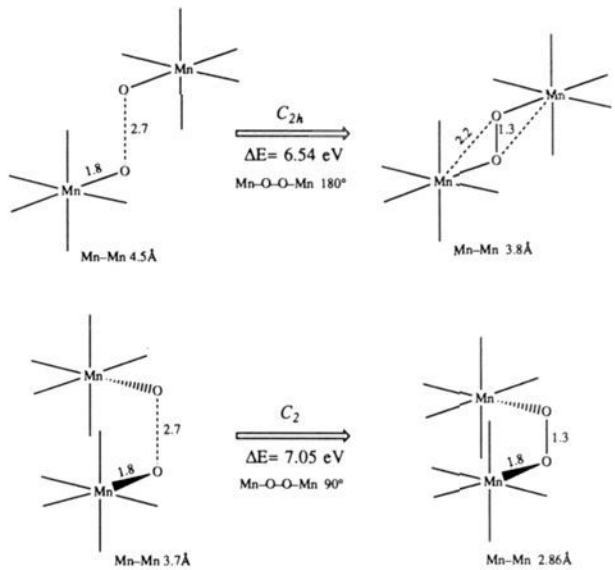

Figure 5. Approach of two $MnOL_5$ monomers leading to oxygen coupling.

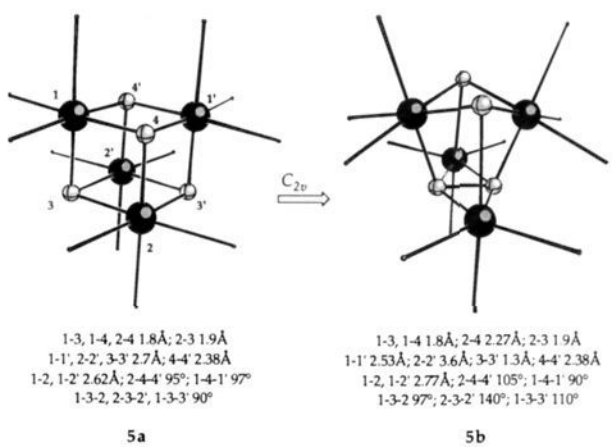

Figure 6. Tetranuclear Mn cluster (cubane-like, **5**) as model for the $S_3 \rightarrow [S_4]$ transition in PSII.

O–O bond formation step may start already from a distorted geometry.

Now we are ready to model different tetramers of manganese, using the dimers as building blocks. The possible combinations are enormous, but again we are guided by the known inorganic complexes. At the same time our results on the oxygen coupling in dimers allow us to reduce the number of possible models.

The first geometry examined follows the hypothesis of a symmetric cubane-like core as a reactive center of PSII.[20] We can easily build such a model (**5a,b**) combining together two dimers **4a**; the four μ-oxo bridges become μ_3-oxo. Now we compute a

(18) (a) Baumgarten, M.; Tso, J.; Marino, J.; Sivaraja, M.; Lin, C. P.; Dismukes, C.; Sheats, J. E.; Gast, P.; Philo, J. S. In *Proceedings of the 8th International Congress on Photosynthesis*; Baltscheffsky, M., Ed.; Kluwer Press: Dordrecht, 1990; (b) *Biophys. J.* **1990**, *57*, 571a. (c) Dismukes, C.; Sheats, J. E.; Mathur, P.; Czernuszewicz, R. In *Proceedings of the 7th International Congress on Photosynthesis*; Baltsheffsky, M., Ed.; Kluwer Press: Dordrecht, 1987.

(19) Bossek, U.; Weyhermüller, T.; Wieghardt, K.; Nuber, B.; Weiss, J. *J. Am. Chem. Soc.* **1990**, *112*, 6387–6388. The first peroxo complex of Mn has been observed in a trinuclear cluster; see: Bhula, R.; Gaisford, G. J.; Weatherburn, D. C. *J. Am. Chem. Soc.* **1988**, *110*, 7550–7552.

(20) (a) Brudvig, G. W.; Crabtree, R. H. *Proc. Natl. Acad. Sci. U.S.A.* **1986**, *83*, 4586–4588. We have not examined the "adamantane" to "cubane" rearrangement mechanism proposed in this paper. EXAFS data argue against such a high-symmetry mechanism (ref 7). (b) Christou, G.; Vincent, J. B. *Biochim. Biophys. Acta* **1987**, *895*, 259–274. (c) Wang, S.; Folting, K.; Streib, W. E.; Schmitt, E. A.; McCusker, J. K.; Hendrickson, D. N.; Christou, G. *Angew. Chem., Int. Ed. Engl.* **1991**, *30*, 305–306.

Table II. Selected Overlap Populations (op) and Net Charges (nc) for the Structures Reported in Figures 5–7

model		op Mn–O	op O–O	nc Mn	nc O	ΔE (eV)
5a–5b	cubane-like C_{2v}	0.38/0.41[a] 0.30/0.23[d]	0.00/0.52[b]	+1.1/+0.53[c] +1.00/+0.82[e]	−0.85/+0.04[b]	5.44
6a–6b	O_2 in-plane D_{2h}	0.45/0.45[a,d] 0.40/0.37[f]	0.00/0.52[b]	+0.90/+0.50[c,e]	−1.02/−0.06[b]	4.25
6a–7	O_2 out-of-plane C_{2v}	0.45/0.40[a,d] 0.40/0.41[f]	0.00/0.53[g]	+0.90/+0.42[c,e]	−1.09/−0.01[g]	5.40
8a–8b	planar T C_{2v}	0.44/0.47[a] 0.44/0.30[d]	0.00/0.52[b]	+0.90/+0.43[e] +1.10/+0.75[h] +0.75/+0.27[i]	−1.04/−0.10[b]	4.38

[a] For atoms 1–3 and 1′–3′. [b] For atoms 3–3′. [c] For atoms 2 and 2′. [d] For atoms 2–3 and 2′–3′. [e] For atoms 1 and 1′. [f] For atoms 1–4 and 2–4′. [g] For atoms 4–4′. [h] For atom 2. [i] For atom 5.

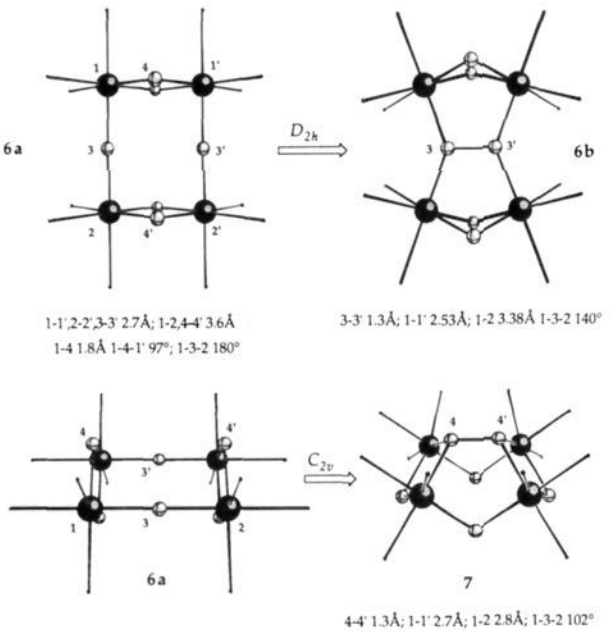

Figure 7. Tetranuclear Mn clusters (O_2 in-plane, **6**, and O_2 out-of-plane, **7**) as models for the $S_3 \rightarrow [S_4]$ transition in PSII.

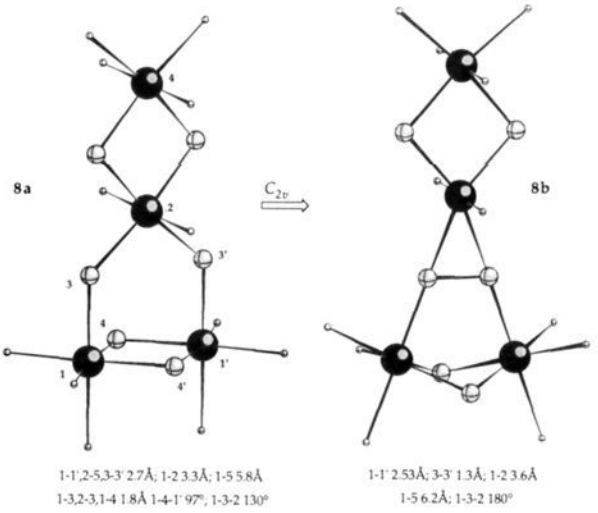

Figure 8. Tetranuclear Mn clusters (planar T, **8**) as models for the $S_3 \rightarrow [S_4]$ transition in PSII.

distortion that combines the more stable ones found for the dimers: **1a–1b** and **4a–4b**. In Figure 6 the lower fragment (2,2′,3,3′ in **5a**) distorts within a plane like the model **1a–1b**, while the upper fragment (1,1′,4,4′,3,3′) distorts out of plane as in **4a–4b**.

The second model (**6a,b**) mimics the μ_4,η^2-O_2 coordination proposed by Lippard and co-workers[21a–c] from the analogy with a synthetic tetrairon cluster in which two oxygens lie in the center of a rectangle of irons, coordinated to all four metals. The analogous clusters of manganese have been isolated recently: a "dimer-of-dimers" of **6a** type $[(Mn_2(\mu\text{-}O)_2)_2L_2]^{4+}$,[22a] and a tetranuclear cluster with O_2 in an in-plane coordination similar to **6b** with μ_4,η^2-O_2H.[22b] In Figure 7 we show how the combination of two distortions of type **4a–4b** can reach the μ_4,η^2-O_2 coordination. The resulting Mn_4O_2 **6b** unit is kept planar along the distortion, the only change being the 3–3′ distance. Starting from the same complex **6a**, we distort the molecule out-of-plane, forming a different tetracoordination **7**, as shown in Figure 7. The latter geometry (**7**) was recently suggested by Lippard and co-workers[21b] for the S_4 state that minimizes the barrier to triplet oxygen formation (vide infra). Another combination of dimers is possible that has no analogous inorganic Mn complex.[23] Model **8a–8b**, illustrated in Figure 8, explores the possibility of a "planar T" tetranuclear cluster formed by an orthogonal pair of Mn_2O_2 units. Some selected results for the four clusters are reported in Table II. The charges show that this peroxo-bound intermediate is consistent with the thermodynamics of two-electron transfer.[5] From the lower ΔE we select **6b** and **8b** as candidates for the $[S_4]$ state in the water oxidation cycle. It is evident that a lower barrier is obtained for the in-plane pathway. Comparing the overlap populations, it appears that the Mn–O bonds are not simply related to the energy barrier. The O–O op are almost equal for the three tetranuclear models. To weaken the Mn–O bond, the Mn–Mn distance should be lengthened (as in **1a–1b** and **5a–5b**) or the O_2 unit should be formed out-of-plane (as in **2a–2b** and **7**) or asymmetrically coordinated as in **8a**. This is directly related to the question of how oxygen is released from $[S_4]$ to reach S_0. If the *postulate* first proposed by Renger is valid, the dioxygen is released spontaneously from $[S_4]$ in an exothermic ligand exchange with two water molecules.[24] This "exoergonic ligand–ligand exchange"[24a] may donate the energy necessary to break the Mn–O bonds. Other calculations suggest that this is the rate-limiting step.[25]

Now we come to the question of how to correlate the spin state of the peroxo complex with the spin state of molecular oxygen released after O–O bond formation. Direct measurement of PSII by magnetic susceptibility has found the O_2 to be in the ground (triplet) state, and that is the case within 10 ms of the O_2 release.[26] We have considered four possible μ-peroxo-$\kappa O{:}\kappa O'$ intermediates: three C_{2v} complexes (**5b**, **7**, and **8b**) and a D_{2h} complex (**6b**) with the two levels descending from the π_g^* of O_2, both doubly occupied.

(21) (a) Micklitz, W.; Lippard, S. J. *Inorg. Chem.* **1988**, *27*, 3069–3075. (b) Micklitz, W.; Bott, S. G.; Bentsen, J. G.; Lippard, S. J. *J. Am. Chem. Soc.* **1989**, *111*, 372–374. (c) Bentsen, J. G.; Micklitz, W.; Bott, S. G.; Lippard, S. J. *J. Inorg. Biochem.* **1989**, *36*, 226.

(22) (a) Chan, M. K.; Armstrong, W. H. *J. Am. Chem. Soc.* **1991**, *113*, 5055–5057. (b) Stibrany, R. T.; Gorum, S. M. *Angew. Chem., Int. Ed. Engl.* **1990**, *29*, 1156–1157.

(23) A similar structure has been identified for the oxygen binding site in a multicopper protein ascorbate oxidase; see: Messerschmidt, A.; Rossi, A.; Ladenstein, R.; Huber, R.; Bolognesi, M.; Gatti, G.; Marchesini, A.; Petruzzelli, R.; Finazzi-Agrò, A. *J. Mol. Biol.* **1989**, *206*, 513–529.

(24) (a) Renger, G. *FEBS Lett.* **1977**, *81*, 223–228. (b) Kambara, T.; Govindjee. *Proc. Natl. Acad. Sci. U.S.A.* **1985**, *82*, 6119–6123.

(25) Anderson, A. B.; Awad, M. K. *J. Am. Chem. Soc.* **1989**, *111*, 802–806.

(26) Philo, J. S.; Gast, P.; Khangulov, S. V.; Tang, X.-S.; Dismukes, G. C. *Biochemistry*, submitted for publication.

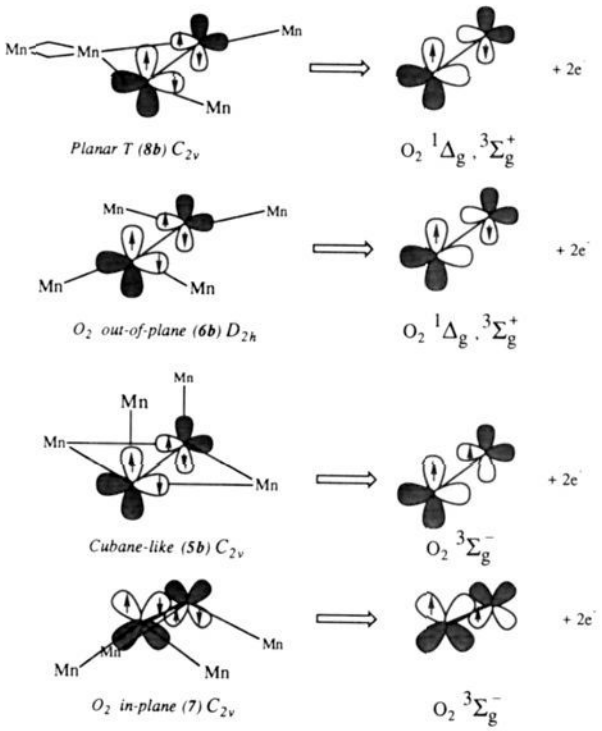

Figure 9. Correlation of the O_2 states for the tetranuclear Mn cluster in the $[S_4] \rightarrow S_0$ transition.

The remaining two-electron reduction of manganese by bound peroxide proposed to take place during $[S_4] \rightarrow S_0$ may be examined with a qualitative localized valence bond picture.

In Figure 9 (top) we correlate the two levels from the π_g^* in D_{2h} model **6b** and C_{2v} model **8b** with the O_2 excited state $(\pi_x^*)^2(\pi_y^*)^0$, simply by removing the four D_{2h} or three C_{2v} Mn atoms along the Mn–O bond directions. Only one of the π_g^* levels interacts with the Mn atoms, and this is predicted to be the level from which the remaining two electrons are removed to form O_2. In **5b** and **7** (C_{2v} symmetry) the four Mn atoms interact with both π_g^*, correlating with the O_2 ground-state triplet $(\pi_x^*)^1(\pi_y^*)^1$ (Figure 7, top and bottom). The first excited singlet state of oxygen lies ~1 eV above the ground triplet state. To remove the excited oxygen from **6b** or **8b**, we need to overcome an electronic barrier of ~1 eV. This increases the ΔE of formation of complexes **6b** (O_2 in-plane) and **8b** (planar T) close to the barrier computed for **5b** and **7**. But this distortion is improbable for **6b**. Four Mn atoms would not move out simultaneously. More likely, the **6b** structure would distort to **7**. So the activation energy must be paid either way, as the added electron energy of the singlet O_2 or as geometrical distortion to move from **6b** to **7**. It follows that all four models are possible candidates for $[S_4]$, but the XAS results[7] help us to select among them. In Table III we collect different Mn–Mn distances for the three models. Comparing with Table II we see immediately that the cubane-like structure is less likely to be a good model, because of its high symmetry, as already suggested.[7d,e] The reader's attention is directed toward a relevant discussion of O_2 evolution by Nishida,[27a] stressing the importance of the electronic state of the departing O_2, as well as to the already cited work of Lippard.[21c]

Other possible tetramer models based upon the approach of two Mn_2O_2 units like **1a**, along the coordinate illustrated in Figure 5, also fail to give any lower barrier to formation of bound peroxide than that for the simple dimers.

The computed energy barrier for the tetramers is not that much below the ones calculated for the binuclear models **1a,b** and **4a,b**.

Table III. Mn–Mn Distances (Å) for the Mn Cluster in PSII and the Models in Figures 5–7

spinach PSII or model	S_3	$[S_4]$	$(S_1 + S_2)^a$
cubane-like C_{2v}	2 at 2.62	2 at 2.77	–
5a–5b	1 at 2.70	0.5 at 3.60	–
		0.5 at 2.53	–
O_2 in-plane D_{2h}	1 at 2.70	1 at 2.53	–
6a–6b	1 at 3.60	1 at 3.38	–
	1 at 4.50	1 at 4.23	–
O_2 out-of-plane C_{2v}	1 at 2.70	1 at 2.70	–
6a–7	1 at 3.60	1 at 2.80	–
	1 at 4.50	1 at 3.89	–
planar T C_{2v}	1 at 2.70	0.5 at 2.53	–
8a–8b		0.5 at 2.70	
	1 at 3.28	1 at 3.60	–
	1 at 5.85	1 at 6.20	–
spinach PSII	–	–	1–1.5 at 2.7[b]
	–	–	0.5 at 3.3 (Mn or Ca)[b]

[a] Sauer et al.[7g] [b] George et al.[7a] report 1.3–2.9 at 2.7 Å and 0.5–1.1 at 3.3 Å; Penner-Hahn et al.[7d] report 1–1.5 at 2.7 Å, 0.5–1 at 3.3 Å, and 0.5 at 4.3 Å (Mn or Ca).

Why are the tetranuclear models preferred? As already noted, to form a full O=O double bond, we have to remove two electrons from MOs with π_g^* character. The $\pi_g^*(z)$ contributes mainly (77%) to the level that lies immediately below the d-block (see Figure 2). This level is largely centered on the oxygens, with Mn–O bonding character, as shown in Figure 3, center. The remaining 23% mixes with the metal d-block ("t_{2g}"), producing a MO mainly centered on the Mn, with Mn–O and O–O antibonding character. This level is pushed up more for the tetranuclear models than for the dimers by 0.3–0.6 eV. Therefore, the barrier for the removal of the two electrons from the MO with π_g^* character is lowered by the same amount. Consequently, the dioxygen formation should be slightly preferred for a tetranuclear Mn cluster.

We are aware that a barrier of 4.25 eV is still much too large, but it should be considered as approximate and evaluated in the context of numbers for different models given by the same theoretical procedure. Other computations, including spin-pairing energy, proton transfer, and the effect of the protein environment, will eventually give more reliable numbers. But the current state of quantum chemical theory does not yet approach the reliability that is needed to definitively identify transition states.

It should be noted here that some ab initio calculations[28] were carried out by other workers in order to analyze the coupling of the oxidation with proton transfer from a coordinated water molecule, using a model of $Mn(H_2O)_5^{n+}$. Recent experimental studies on di-μ-oxo Mn dimers show the coupling of proton ionization (hydrogen transfer) from a bridging hydroxo ligand to a reversible one-electron oxidation.[29]

Recent observations suggest an important role for Ca^{2+} and Cl^- in photosystem II.[3,30,31] The substitution of some ligands with Cl^- or imidazole does not influence the energetics of the oxygen coupling for our models. The effect of both ions cannot be easily computed within the extended Hückel formalism.

(27) (a) Nishida, Y. *Inorg. Chim. Acta* **1988**, *152*, 73–74. (b) A model to explain the magnetic properties of PSII has been proposed recently: Nishida, Y.; Nasu, M. *Z. Naturforsch. C* **1990**, *45c*, 1004–1010.

(28) (a) Kusunoki, M.; Kitaura, K.; Morokuma, K.; Nagata, C. *FEBS Lett.* **1980**, *117*, 179–182. (b) Kusunoki, M. In *The Oxygen Evolving System in Photosynthesis*; Inoue, Y., Crofts, A. R., Govindjee, Murata, N., Renger, G., Satoh, K., Eds.; Academic Press: Japan, 1983; pp 165–173. (c) Kusunoki, M. In *Advances in Photosynthesis Research*; Sybesma, C., Ed.; Nijhoff/Junk Pub.: Dordrecht, 1984; Vol. 1, pp 275–278.

(29) (a) Cooper, S. R.; Calvin, M. *J. Am. Chem. Soc.* **1977**, *99*, 6623–6629. (b) Thorp, H. H.; Sarneski, J. E.; Brudvig, G. W.; Crabtree, R. H. *J. Am. Chem. Soc.* **1989**, *111*, 9249–9250. (c) Manchanda, R.; Thorp, H. H.; Brudvig, G. W.; Crabtree, R. H. *Inorg. Chem.* **1991**, *30*, 494–497.

(30) (a) Miller, A.-F.; Brudvig, G. W. *Biochemistry* **1989**, *28*, 8181–8190. (b) Boussac, A.; Rutherford, A. W. *Biochemistry* **1988**, *27*, 3476–3483. (c) Homann, P. H. *J. Bioenerg. Biomembr.* **1987**, *19*, 105–123.

(31) (a) Coleman, W. J. *Photosynth. Res.* **1990**, *23*, 1–27. (b) Wydrzynski, T.; Baumgart, F.; MacMillan, F.; Renger, G. *Photosynth. Res.* **1990**, *25*, 59–72. (c) Baumgarten, M.; Philo, J. S.; Dismukes, G. C. *Biochemistry* **1990**, *29*, 10814–10822.

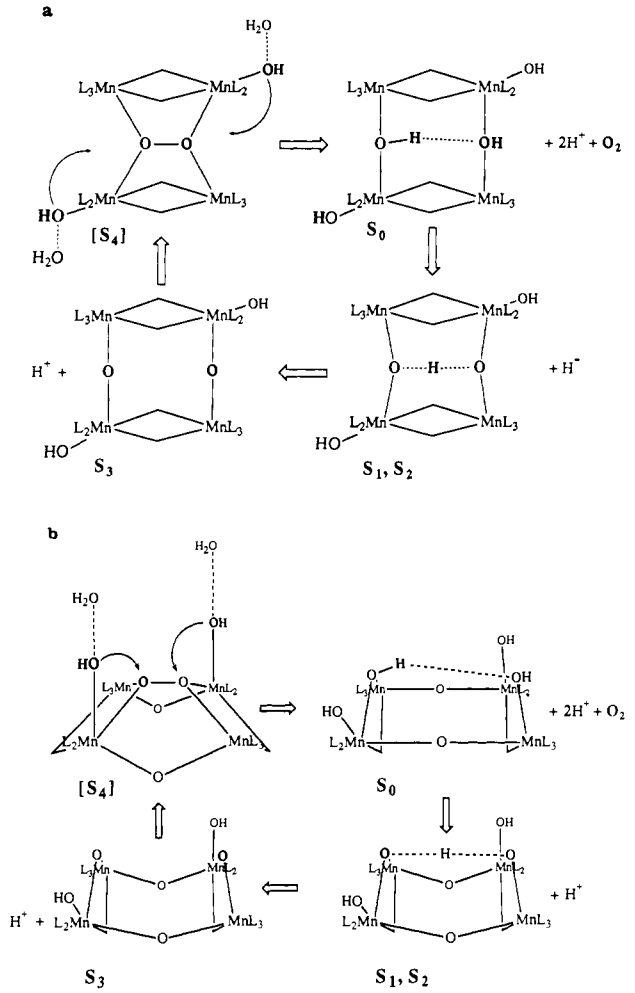

Figure 10. (a) Proposed PSII cycle for the model **6a–6b**. (b) Proposed PSII cycle for the model **6a–7**.

We can now propose a possible mechanism that correlates the two models for the $[S_4]$ state with the entire cycle (I).[27b] We couple each step from S_0 to $[S_4]$ with the appropriate proton transfer,[4,32] and by following the XAS results, we draw two possible mechanisms, one for the in-plane oxygen coupling **6a–6b** (see Figure 10a) and one for the out-of-plane **6a–7** (see Figure 10b). A mechanism equivalent to Figure 10a can be drawn easily for the "planar T" model **8a–8b**. This geometry is also consistent with a low-energy mechanism. It must be noted that these mechanisms do not include the energetics of proton release in a quantitative sense and are highly speculative.

Starting from $[S_4]$, the oxygen must be removed. To achieve S_0 two steps should be taken at the same time: removal of O_2 and introduction of two water molecules as new ligands. The simplest way to do this is to replace the dioxygen, by bending two axial OH^- ions, while two water molecules approach along the same direction as the axial ligands, with a total release of two H^+ ions. A concerted mechanism would minimize the activation energy involved in the breaking and making of Mn–O bonds. The product is a possible candidate for S_0. In Figure 10a,b some of the oxo bridges are shown as linear for S_0, but those bridges have great flexibility. In the inorganic structures known the Mn–O–Mn angle varies from 90° to 180°.[33] The role of hydrogen bonding

Table IV. Atomic Parameters Used in the Calculations

atom	orbital	H_{ii} (eV)	ζ_1	ζ_2	C_1[a]	C_2[a]
Mn	4s	−9.88	1.80			
	4p	−5.45	1.80			
	3d	−12.53	5.15	1.90	0.53108	0.64788
O	2s	−32.3	2.275			
	2p	−14.8	2.275			
H	1s	−13.6	1.30			

[a] Coefficients in double-ζ expansion.

in this hypothesis is to fix the geometry for PSII in the range of distances observed with XAS studies. From S_0, the stable S_1 state could be reached easily, coupling the deprotonation of the bridge with the formation of a stronger intermolecular hydrogen bond. The geometries of S_0, S_1, and S_3 in Figure 10a,b are similar to those proposed by Lippard and co-workers[21,34] and to the inorganic analogues in ref 22. The hydrogen bond brings the oxo atoms closer for the next step, where another electron is removed, forming the S_2 state. A further oxidation and deprotonation bring one to the S_3 state. These are the appropriate oxidation-state models for the $S_1 \rightarrow S_2$ and $S_2 \rightarrow S_3$ transitions. In the S_3 state the O–O bond is not yet formed and the geometry of the oxo bridges allows small changes on moving from S_2 to S_3. The last oxidation step is proposed to create significant electron removal from the μ-oxo ligands and promote bending of the two bridges forming the O–O peroxo bond in the nascent $[S_4]$ state, without proton release. The cycle is completed by removal of the two remaining π_g^* electrons to form dioxygen and reduce manganese.

Some of the features of these models can be justified as follows. The most recent XAS results suggest asymmetric coordination in S_1 and S_2 states like that illustrated in V.[7g] It is a simple extrapolation to convert this open structure to the more symmetric closed structures like those in **6a** and **8a** for the nascent $[S_4]$ state.

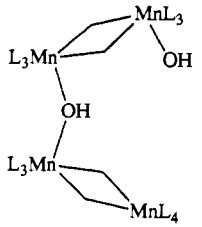

V

The proposed ionization of the hydrogen-bonded μ-hydroxo in the $S_1 \rightarrow S_2$ or $S_2 \rightarrow S_3$ transitions can be suggested on the basis of model complexes showing a decrease in the pK_a from 11 to 2.3 for the μ-hydroxo group found in the $Mn^{III}{}_2 \rightarrow Mn^{III}Mn^{IV}$ oxidation step.[29]

Conclusions

The results of our analysis of the molecular mechanism of photosynthetic oxygen evolution are summarized as follows. The tri- or tetracoordination of peroxide slightly lowers the energy for the two-electron oxidation to dioxygen by destabilization of the $\pi_g^*(z)$ orbitals on the O_2 unit. The in-plane approach of two oxo atoms has a lower energy barrier for peroxide formation, but correlates with release of singlet dioxygen, not ground-state triplet. Large energy barriers are calculated when starting from equilibrium structures for manganese clusters such as those reported in the literature. None of these are known to be active in water oxidation. This suggests that activation of oxygen in photosystem II may be created by distorted coordination of water ligands far from the equilibrium structures seen for synthetic manganese oxo complexes.

Acknowledgment. We thank the Consiglio Nazionale delle Ricerche (CNR, Italy) for the award of a postdoctoral fellowship

(32) Nonstoichiometric proton ionization results have been reported recently: Johns, P.; Lavergne, J.; Rappaport, F.; Junge, W. *Biochim. Biophys. Acta* **1991**, *1057*, 313–319.

(33) (a) Caneschi, A.; Ferraro, F.; Gatteschi, D.; Melandri, M. C.; Rey, P.; Sessoli, R. *Angew. Chem., Int. Ed. Engl.* **1989**, *28*, 1365–1367. (b) Chan, M. K.; Armstrong, W. H. *J. Am. Chem. Soc.* **1989**, *111*, 9121–9122. (c) Kipke, C. A.; Scott, M. J.; Gohdes, J. W.; Armstrong, W. H. *Inorg. Chem.* **1990**, *29*, 2193–2194. (d) Chan, M. K.; Armstrong, W. H. *J. Am. Chem. Soc.* **1990**, *112*, 4985–4986.

(34) Bentsen, J. G.; Micklitz, W.; Lippard, S. J. Unpublished results.

to D.M.P., the National Science Foundation for its support through Grant CHE-8912070 to R.H., and the National Institutes of Health for support under Grant GM-39932.

Appendix

For the computations we use the extended Hückel method,[35] a semiempirical molecular orbital procedure, with weighted H_{ij}'s.[36] The parameters used in the calculations are reported in Table IV. For the H_{ii} of Mn we carried out a charge-iteration calculation on $[Mn(H_2O)_6]^{2+}$, O_h with Mn-O 2.1 Å. This choice produces reasonable atomic net charges for the tetranuclear models **6** and **7** (see Table II). Charge iteration for Mn in a higher oxidation state should produce a contraction of the atomic orbitals (the exponents ζ of the Slater-type orbitals become bigger) and lower the H_{ii} (valence-orbital ionization potential). The use of a different set of parameters for higher oxidation states of Mn does not qualitatively change our results. The three-dimensional graphics have been carried out by a computer program named CACAO, described elsewhere.[37]

Registry No. O_2, 7782-44-7; Mn, 7439-96-5.

(35) Hoffmann, R.; Lipscomb, W. N. *J. Chem. Phys.* **1962**, *36*, 2179, 3489. Hoffmann, R. *J. Chem. Phys.* **1963**, *39*, 1397.
(36) Ammeter, J. H.; Bürgi, H.-B.; Thibeault, J. C.; Hoffmann, R. *J. Am. Chem. Soc.* **1978**, *100*, 3686.
(37) Mealli, C.; Proserpio, D. M. *J. Chem. Educ.* **1990**, *66*, 399.

Topological Properties of Electron Density in Search of Steric Interactions in Molecules: Electronic Structure Calculations on Ortho-Substituted Biphenyls

Jerzy Cioslowski* and Stacey T. Mixon

Contribution from the Department of Chemistry and Supercomputer Computations Research Institute, Florida State University, Tallahassee, Florida 32306-3006. *Received August 26, 1991*

Abstract: The bond critical points in the electron density are not necessarily associated with bonding interactions. When the distance between two atoms is smaller than their contact interatomic separation (CIS), an attractor interaction line passing through the corresponding bond critical point appears, indicating a nonbonding repulsive interaction. Sterically crowded molecules are defined as those possessing such interaction lines at their equilibrium geometries. The appearance (or disappearance) of the interaction lines along the reaction paths allows for classification of the barriers to rotation into the categories of those sterically hindered, sterically facilitated, and sterically neutral. The values of contact interatomic separations provide a measure of the steric crowding in molecules that is, due to its mathematical rigor, superior to the concept of the van der Waals radii. The HF/6-31G** electronic structure calculations on biphenyl and its ortho-substituted derivatives illustrate the applications of the aforementioned theoretical concepts.

Introduction

Among many concepts often taken for granted by chemists is that of a chemical bond. For a large fraction of the molecules currently known, chemical intuition aids in assigning the bonding patterns. However, making intuitive decisions about which atoms are linked through chemical bonds becomes a confusing and error-prone task once less common chemical systems are considered. The case of organolithiums[1,2] can serve as a good example of the difficulties encountered in making unequivocal bond assignments without a formal definition of the chemical bond.

In principle, one might derive the bonding patterns from knowledge of bond orders. However, such an approach is of limited value, as an arbitrary cutoff would have to be decided upon to determine what magnitude of the bond order is sufficient to make a pair of atoms linked by a bond. Moreover, most of the currently used bond orders and indices[3,4] are based on a partitioning of the Hilbert space spanned by basis functions used in ab initio calculations, which brings further (unnecessary) lack of rigor. The same is true about some other schemes that find optimal locations of chemical bonds.[5]

The electronic wave function of any chemical system contains all the information about its electronic structure. Therefore, one cannot imagine any formal definition of bonding universally applicable to all molecules not taking the relevant characteristics of the electronic wave function into account. The link associating the electronic wave function and chemical bonds is not as elusive as one might think. In fact, as demonstrated by Bader,[6,7] the knowledge of the electron density, $\rho(\vec{r})$, is sufficient to define the bonding pattern of any molecule. In order to accomplish that, the critical (extremal or stationary) points, at which the gradient of $\rho(\vec{r})$ vanishes

$$\vec{\nabla}\rho(\vec{r}_{crit}) = 0 \qquad (1)$$

are located first. The extremal points characterized by two negative and one positive eigenvalues of the Hessian matrix **h**

$$h_{pq} = \frac{\partial}{\partial p}\frac{\partial}{\partial q}\rho(\vec{r})|_{\vec{r}=\vec{r}_{crit}} \qquad p, q = x, y, z \qquad (2)$$

are known as the bond points, whereas those with two positive eigenvalues are called ring points. At each bond point, two gradient paths (the lines of steepest ascent in $\rho(\vec{r})$), known collectively as the attractor interaction lines, originate. The attractor

(1) Ritchie, J. P.; Bachrach, S. M. *J. Am. Chem. Soc.* **1987**, *109*, 5909.
(2) Cioslowski, J. *J. Am. Chem. Soc.* **1990**, *112*, 6536.
(3) Wiberg, K. B. *Tetrahedron* **1968**, *24*, 1083.
(4) Mayer, I. *Chem. Phys. Lett.* **1984**, *110*, 440.
(5) Reed, A. E.; Weinhold, F. *J. Chem. Phys.* **1985**, *83*, 1736.
(6) Bader, R. F. W. *Atoms in Molecules: A Quantum Theory*; Clarendon Press: Oxford, U.K., 1990.
(7) Bader, R. F. W. *Acc. Chem. Res.* **1985**, *18*, 9.

0002-7863/92/1514-4382$03.00/0